The Canadian Mineralogist
Vol. 46, pp. 1033-1042 (2008)
DOI: 10.3749/canmin.46.4.1033

FLUORINE-RICH HIBSCHITE FROM SILICOCARBONATITE, AFRIKANDA COMPLEX, RUSSIA: CRYSTAL CHEMISTRY AND CONDITIONS OF CRYSTALLIZATION

ANTON R. CHAKHMOURADIAN§ AND MARK A. COOPER

Department of Geological Sciences, University of Manitoba, Winnipeg, Manitoba R3T 2N2, Canada

LUCA MEDICI

Istituto di Metodologie per l'Analisi Ambientale, Tito Scalo, I–85050 Potenza, Italy

FRANK C. HAWTHORNE

Department of Geological Sciences, University of Manitoba, Winnipeg, Manitoba R3T 2N2, Canada

FRAN ADAR

Molecular and Microanalysis Division, Horiba Jobin Yvon, Edison, New Jersey 08820, U.S.A.

ABSTRACT

Calcite – amphibole – diopside silicocarbonatite from the Afrikanda complex, in the Kola Peninsula, northwestern Russia, contains abundant crystals of F-rich hibschite associated with titanite, chlorite, calciocatapleiite and calcite. The crystals range from 10 to 50 μm across and consist of an oscillatory-zoned core and a uniform rim arising from variations in Al and Fe contents across the crystal. The hibschite contains from 4.2 to 6.0 wt.% F, which is unparalleled by any F-bearing silicate garnet described to date. The compositional variation of the Afrikanda hibschite can be described by the formula $Grs_{57–63}Kt_{21–27}Fgr_{8–11}Adr_{0–13}$, where Grs, Kt and Adr stand for the grossular, katoite and andradite, respectively, and Fgr denotes the hypothetical end-member $Ca_3Al_2F_{12}$.The average Fgr content is 10 mol.%. The crystal structure of F-rich hibschite was refined in space group $Ia\bar{3}d$ to R_1 = 2.8%. In agreement with the chemical data, the refinement shows that about one-third of the tetrahedrally coordinated positions (*Z*) are vacant. These vacancies are coordinated by $(OH)^-$ and F^- anions, which results in expansion of the unit cell [*a* = 12.037(3) Å] relative to that of grossular. The size of the *Z*-centered tetrahedron is sensitive to the substitution of $(OH)^-$ by F^-, as indicated by the smaller center-to-corner and corner-to-corner distances measured for the Afrikanda hibschite relative to garnets with a similar Si content along the grossular–katoite join. The F-rich hibschite crystallized in the final stages of silicocarbonatite evolution from a low-temperature (200–250°C) deuteric fluid with $\log a(H^+)_{aq} \approx \log a(F^-)_{aq} \approx -5$.

Keywords: hibschite, F-rich garnet, crystal structure, silicocarbonatite, Afrikanda complex, Kola Peninsula, Russia.

SOMMAIRE

La silicocarbonatite à calcite, amphibole et diopside du complexe de Afrikanda, dans la péninsule de Kola en Russie, contient une abondance de cristaux de hibschite riche fluor associés à la titanite, chlorite, calciocatapléiite et calcite. Les cristaux vont de 10 à 15 μm de diamètre et possèdent un noyau à zonation oscillatoire et une bordure uniforme, résultats de variations en teneurs de Al et Fe. La hibschite contient de 4.2 à 6.0% de F (en poids), ce qui est sans égal parmi les exemples connus de grenat silicaté fluoré à date. On peut décrire la variation en composition de la hibschite de Afrikanda par la formule $Grs_{57–63}Kt_{21–27}Fgr_{8–11}Adr_{0–13}$ $Grs_{57–63}Kt_{21–27}Fgr_{8–11}Adr_{0–13}$, dans laquelle Grs, Kt et Adr représent les pôles grossulaire, katoite et andradite, respectivement, et Fgr représente le pôle hypothétique idéal $Ca_3Al_2F_{12}$. La teneur moyenne en Fgr est 10% (base molaire). Nous avons affiné la structure cristalline de la hibschite fluorée dans le groupe spatial $Ia\bar{3}d$ jusqu'à un résidu R_1 de 2.8%. En concordance avec les données chimiques, l'affinement montre qu'environ un tiers des positions Z à coordinence quatre sont vides. Ces lacunes sont coordonnées par des groupes $(OH)^-$ et des anions F^-, ce qui mène à une expansion de la maille élémentaire *a* à 12.037(3) Å, relative à la valeur pour le grossulaire. La dimension du tétraèdre est sensible à la substitution du $(OH)^-$ par F^-, comme l'indique les distances plus courtes du centre Z aux coins et de coin à coin par rapport à celles des échantillons de grenat de la série grossulaire–

§ *E-mail address*: chakhmou@cc.umanitoba.ca

katoite ayant une teneur en Si semblable. La hibschite riche en fluor a cristallisé au stade final de l'évolution de la silicocarbonatite à une faible température (200 à 250°C) a partir d'une phase fluide dans laquelle log $a(H^+)_{aq} \approx$ log $a(F^-)_{aq} \approx -5$.

Mots-clés: hibschite, grenat riche en fluor, structure cristalline, silicocarbonatite, complexe de Afrikanda, péninsule de Kola, Russie.

Introduction

Calcic garnets are common accessory constituents of silicocarbonatites and primitive calcite carbonatites enriched in autolithic or xenolithic silicate material. To date, there has not been a systematic study of calcic garnets from carbonatitic rocks. A few attempts have been made to use these minerals as tracers of magma evolution (*e.g.*, Lupini *et al.* 1992, Brod *et al.* 2003), but those authors relied exclusively on results of electron-microprobe analysis as the basis for petrogenetic interpretations. The shortcomings of this simplified approach were discussed in detail by Chakhmouradian & McCammon (2005). It has been recently recognized that evolution of calcic garnets in some carbonatites culminates with the appearance of a "hydrogarnet" late in the paragenetic sequence (Chakhmouradian & Zaitsev 2002). Such garnet, containing a significant proportion of OH in its chemical composition, precipitates from deuteric hydrothermal fluids either independently or as a reaction-induced mantle on earlier-crystallized minerals (including primary Ca–Fe–Ti garnet, perovskite, titanite and ilmenite). During a systematic study of silicocarbonatites from the Afrikanda complex in the Kola Peninsula, northwestern Russia, we identified in these rocks abundant crystals of calcic "hydrogarnet" containing a high proportion of F. The scarcity of published information on naturally occurring F-bearing garnet in general and "hydrogarnet" from carbonatitic parageneses in particular prompted a detailed investigation of the Afrikanda material. In the present work, we describe the crystal chemistry of a garnet-group mineral with the highest F content reported to date, including the first crystal-structure refinement of a F-rich calcic garnet. The only F-rich garnet whose crystal structure has been refined previously is spessartine from the Henderson mine in Colorado (Smyth *et al.* 1990). The data presented here have implications not only for the interpretation of subsolidus processes in carbonatitic systems, but also further our understanding of the crystal chemistry of the garnet group, an important class of technological materials.

Occurrence and Paragenesis

The Afrikanda alkali-ultramafic complex is composed of texturally diverse olivinites and clinopyroxenites cross-cut by minor intrusions of carbonatitic and foidolitic rocks. Calcite – amphibole – diopside silicocarbonatite and associated sövite are common in the central part of the pluton, where they form veins and lenticular bodies in perovskite–magnetite-bearing olivinites, melilite olivinites, wehrlites and coarse-grained clinopyroxenites (Chakhmouradian & Zaitsev 2004). The silicocarbonatite is a coarse-grained rock comprising variable modal proportions of diopside, magnesiohastingsite, calcite, magnetite, perovskite, titanite and chlorite. Some 50 different accessory minerals have been identified in this rock, including such characteristic "carbonatitic" phases as nyerereite, burbankite, ancylite-(Ce), rare-earth- and Nb-rich perovskite, rare-earth-rich zirconolite and calzirtite (Chakhmouradian & Zaitsev 2004, and references therein). Garnet-group minerals are common accessory constituents in both primary and deuteric parageneses, and locally make up a few vol.% of the rock. The earliest garnet to crystallize in the silicocarbonatite is Zr-bearing OH-poor schorlomite, described elsewhere (Chakhmouradian & McCammon 2005). Grains of deuteric garnet are confined to fractures in the primary calcite and associated with chlorite, titanite and Ca–Zr silicates. Most common are fragmented euhedral crystals of F-rich hibschite and random intergrowths of such crystals enclosed in late-stage hydrothermal calcite and calciocatapleiite (Fig. 1; Chakhmouradian & Zaitsev 2004). Locally, the silicocarbonatite contains hundreds of such crystals in one square centimeter. The hibschite crystallized after Al-rich titanite and nearly simultaneously with Nb- and Zr-rich titanite (Chakhmouradian 2004), but prior to late-stage calcite, calciocatapleiite and the bulk of the chlorite.

The crystals of hibschite are colorless, isotropic and range from 10 to 50 μm in the longest dimension. In back-scattered electron (BSE) images, all crystals show the same pattern of zoning, comprising an oscillatory-zoned core and a uniform rim of low average atomic number (AZ). The zoning is also visible in plane-polarized light owing to the comparatively higher index of refraction of the high-AZ (*i.e.*, Fe-rich) material (Fig. 1a). The core consists of 4–5 high-AZ zones and 3–4 low-AZ zones of differing width (Figs. 1b–e); this pattern results from variations in Fe/Al across the core (see below). Some of the crystals exhibit an interrupted oscillatory pattern, which indicates that they were fragmented prior to their mantling by the uniform low-AZ material in the rim (Figs. 1c, e). Thus, the host silicocarbonatite experienced at least two episodes of fracturing, the earliest of which preceded the deposition of the homogeneous rim of hibschite, whereas the second episode occurred after the crystallization

of hibschite, but prior to the precipitation of late-stage calcite, chlorite and catapleiite.

Analytical Techniques

The composition of hibschite (Table 1) was determined by wavelength-dispersive spectrometry (WDS) using an automated Cameca SX 100 electron microprobe operated at 15 keV and 20 nA, with a beam size of 1 μm. Although beam damage was not observed for any of the analyzed points, several selected points were re-analyzed with a beam current of 10 nA and beam size of 5 μm. The element abundances measured with a narrow beam at 20 nA are within the instrumental standard deviation of the values obtained with a larger beam at 10 nA. For example, the F abundances obtained under these different instrumental conditions are within 5% of each other. Given that the width of some of the zones is 5 μm or less (Fig. 1), the smaller beam-size was eventually chosen for analysis. The following standards were employed: albite (Na), andalusite (Al), diopside (Ca and Si), fayalite (Fe), forsterite (Mg), titanite (Ti) and topaz (F), with *K*α analytical lines used for all of these elements. Several other elements were sought, but found not to be present at detectable levels (*i.e.*, 200 ppm for Cr, 400 ppm for Mn, 500 ppm for V, 600 ppm for Nb and Y, and 800 ppm for Zr).

X-ray microdiffraction (μXRD) data were collected *in situ* on the hibschite crystal shown in Figure 1a using a Rigaku D-max Rapid micro-diffractometer, operated at 40 kV and 30 mA. This instrument is equipped with a Cu*K*α source, curved-image-plate detector, flat graphite monochromator, a variety of beam collimators, motorized stage and microscope for accurate positioning of the sample. The motorized stage allows two angular movements (rotation ϕ and revolution ω). The data were collected in reflection mode using various sample-to-beam geometries and operating conditions. Seven datasets were obtained using a 50-μm collimator and collection times from 2–4 hours, including six datasets with both ϕ and ω fixed, and one with a ϕ range of 6°. In addition, a smaller collimator (30 μm) and longer collection-times (15–18 hours) were used to acquire four datasets with ω fixed and ϕ ranging from 0 to 70°. The results obtained with these different acquisition-parameters are mutually consistent. The μXRD data were collected as two-dimensional images and then converted into 2θ–*I* profiles using the Rigaku R-Axis Display software. Because no evidence of symmetry reduction was observed, the μXRD pattern of hibschite (Table 2) was indexed on a cubic $Ia\bar{3}d$ cell. The unit-cell parameter was refined using the UnitCell software (Holland & Redfern 1997).

A small fragment of hibschite was extracted from a polished thin section for a single-crystal X-ray-diffraction study. It was mounted on a Bruker four-circle diffractometer equipped with an Apex 4K CCD detector and a Mo*K*α X-ray source. In excess of a hemisphere of data was collected to 60° 2θ using a frame time of 180 s and a frame width of 0.1°. Diffraction spots were not observed at greater than 40° 2θ, and this upper limit was imposed during the integration of the data frames. Given a diffracting volume of 1.8×10^{-6} mm^3 and an average scattering of $\sim 1e^- \times$ Å^{-3}, we characterize the general weak observance of diffraction data in this case as *normal* and place this combination of crystal volume and scattering potential at the near-practical limit for current CCD detectors operating with a fixed Mo-anode generator. The unit-cell parameter (Table 3) was determined from 249 reflections with $I > 7\sigma(I)$. The struc-

TABLE 1. REPRESENTATIVE COMPOSITIONS OF F-RICH HIBSCHITE

Oxide or element	Core (high-AZ) max.Fe	Core (low-AZ) min.Fe	Rim average†	Rim e.s.d.	Rim range	"Bulk" average
Na_2O wt.%	0.03	0.05	0.03	0.01	0.02-0.04	0.03
CaO	38.22	38.49	39.00	0.34	38.50-39.50	38.67
MgO	0.05	0.07	0.08	0.01	0.06-0.09	0.08
Al_2O_3	19.83	22.21	23.11	0.37	22.44-23.58	22.54
Fe_2O_3	4.55	1.32	0.30	0.35	0.01-1.01	0.98
TiO_2	0.02	0.07	0.01	0.01	0-0.02	0.01
SiO_2	29.21	27.95	26.29	0.68	25.55-27.51	27.30
F	4.25	5.47	5.62	0.31	5.22-6.01	5.43
$O=F_2$	1.79	2.30	2.37			2.29
H_2O‡	5.06	5.43	6.66	0.52	5.80-7.58	5.93
Total	99.43	98.76	98.73			98.68
Na *apfu*	0.004	0.007	0.005			0.004
Ca	2.996	2.993	2.995			2.996
Σ*X*	3.000	3.000	3.000			3.000
Mg	0.006	0.008	0.009			0.009
Al	1.710	1.900	1.952			1.921
Fe^{3+}	0.250	0.072	0.016			0.053
Ti	0.001	0.004	-			-
Σ*Y*	1.967	1.984	1.977			1.983
Si	2.137	2.028	1.884			1.974
F	0.983	1.256	1.274			1.242
H	2.470	2.631	3.189			2.863

† The bulk composition was calculated from the relative volumes occupied by individual zones; ‡ calculated on the basis of stoichiometry, *i.e.*, assuming $H_{apfu} = 4 \times (3 - Si_{apfu} - 0.25 \times F_{apfu})$. Total Fe is expressed as Fe^{3+}; Cr, Mn, V, Nb, Y and Zr were sought, but not detected.

TABLE 2. μXRD PATTERN OF F-RICH HIBSCHITE

I	d_{meas}	d_{calc}	*h k l*	I	d_{meas}	d_{calc}	*h k l*
1	4.913	4.913	1 1 2	17	1.666	1.669	6 4 0
3	4.255	4.255	2 2 0	2	1.639	1.638	3 3 6
3	3.210	3.216	3 2 1	51	1.611	1.608	6 4 2
7	3.002	3.008	4 0 0	10	1.523	1.528	6 5 1
100	2.690	2.691	4 2 0	14	1.504	1.504	8 0 0
7	2.570	2.566	3 3 2	1	1.457	1.459	8 2 0
12	2.457	2.456	2 2 4	20	1.439	1.438	6 5 3
18	2.362	2.360	4 3 1	7	1.346	1.345	8 4 0
30	2.197	2.197	5 2 1	7	1.313	1.313	8 4 2
3	2.131	2.127	4 4 0	5	1.295	1.298	7 6 1
36	1.953	1.952	1 1 6	6	1.283	1.283	6 6 4
4	1.902	1.903	6 2 0	1	1.218	1.216	8 5 3
2	1.777	1.774	6 3 1	2	1.179	1.180	8 6 2
18	1.738	1.737	4 4 4	8	1.119	1.117	8 6 4
1	1.702	1.702	5 4 3				

The values of *d* are quoted in Å.

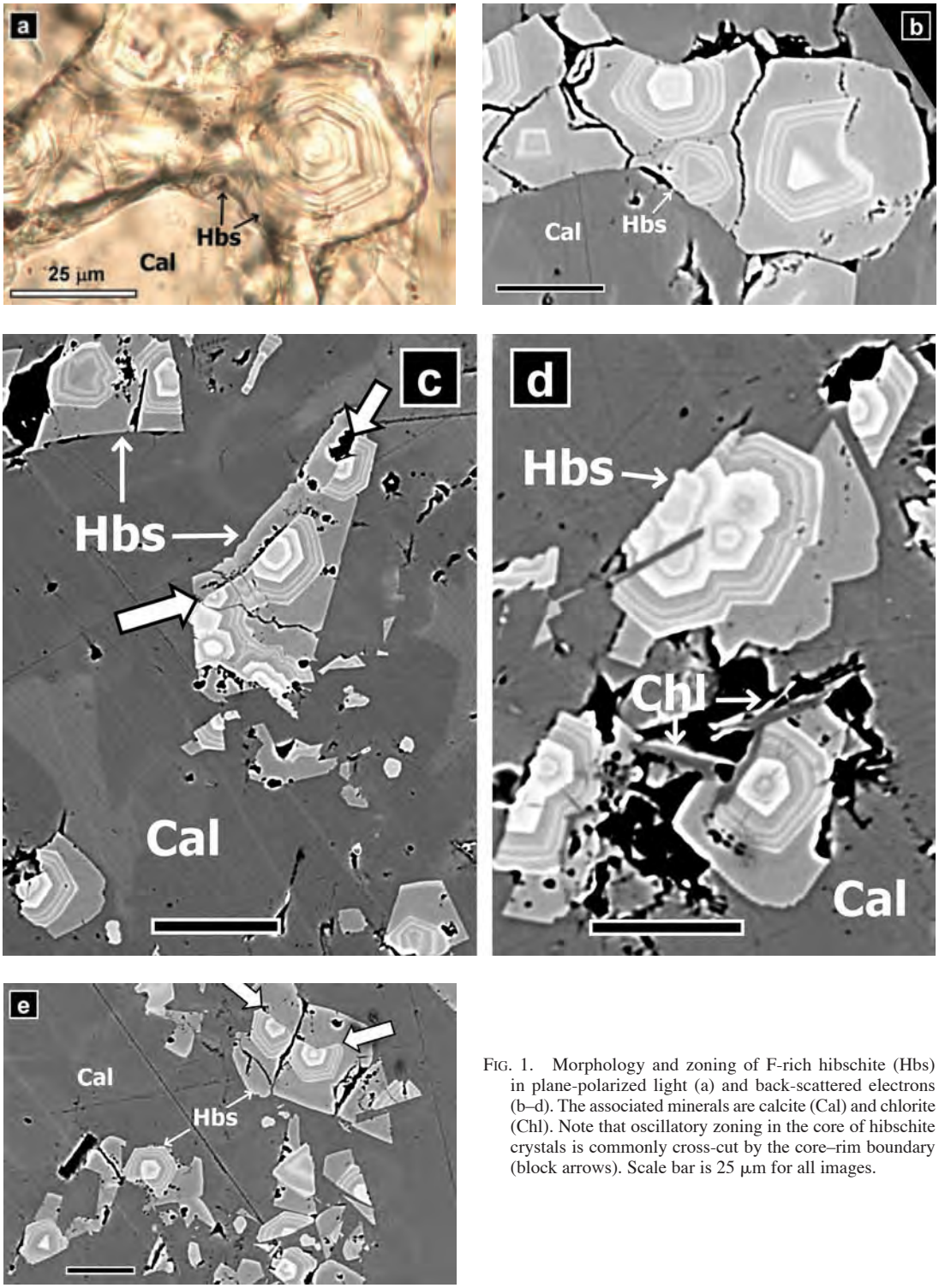

FIG. 1. Morphology and zoning of F-rich hibschite (Hbs) in plane-polarized light (a) and back-scattered electrons (b–d). The associated minerals are calcite (Cal) and chlorite (Chl). Note that oscillatory zoning in the core of hibschite crystals is commonly cross-cut by the core–rim boundary (block arrows). Scale bar is 25 μm for all images.

ture was refined in space group $Ia\bar{3}d$ using the Bruker SHELXTL Version 5.10 package of programs (Sheldrick 1997). Scattering factors were taken from Ibers & Hamilton (1992). Further information pertaining to the single-crystal X-ray data collection and structure refinement is provided in Table 3.

Raman spectra were collected from the crystal shown in Figure 1a using a LabRam HR microspectrometer (Horiba Jobin Yvon) equipped with a 633-nm He–Ne narrow-bandwidth laser and an automated *x*–*y*–*z* stage. Crystalline Si was used as a calibration standard. The spectra were collected in confocal mode in intervals from 100 to 1300 cm^{-1} and 3000 to 3750 cm^{-1} with an 1800 gr/mm grating.

RESULTS

Chemical composition

The oscillatory core of hibschite crystals contains significant, but variable, amounts of Fe and F, whereas their rim is more uniform in composition and contains less Fe and more F relative to the core. The Na, Mg and Ti contents are consistently at or only slightly above the detection limit of WDS (Table 1). Structural formulae, calculated on the basis of three *X*-site cations (Na + Ca), with all Fe cast as Fe^{3+}, invariably give near-stoichiometric cation totals at the *Y* site (1.96–2.01 atoms per formula unit, *apfu*). This observation, coupled with a good antipathetic correlation between the Al and Fe *apfu* values (Fig. 2a), indicates that the bulk of Fe in the examined material is indeed trivalent and replaces Al at the *Y* site. There is also a weak sympathetic correlation between the Al and F contents (Fig. 2b), but no correlation between either Ca and Fe, or Ca and Al. The H_2O content was calculated on the basis of stoichiometry, *i.e.*, assuming $H_{apfu} = 4 \times (3 - Si_{apfu} - 0.25 \times F_{apfu})$, with all Fe cast as Fe^{3+} (Table 1). Cation *apfu* values calculated using this approach give a slightly lower total positive charge relative to the ideal value ($24 - F_{apfu}$). However, the discrepancy does not exceed 0.4%, which is comparable to, or less than, charge discrepancies for "hydrogarnets" described in the literature (*e.g.*, Smyth *et al.* 1990, Ferro *et al.* 2003, Włodyka & Karwowski 2006). Alternatively, the H_2O content in these minerals can be calculated on the basis of charge constraints. In our case, the values determined by the two methods are within 0.2 wt.% of each other in the core of hibschite crystals and within 0.1 wt.% in their rim.

An attempt to quantify the amount of H_2O in the Afrikanda hibschite by synchrotron IR spectroscopy was unsuccessful because of the very small size of the crystals (G. Della Ventura, pers. commun.). The measured Raman spectra clearly show OH-stretching modes near ~3630 cm^{-1} (Fig. 3), but these modes cannot be reliably deconvoluted into components or used to quantify the H_2O content (for a detailed discussion, see Arredondo & Rossman 2002). Variations in intensity of the OH stretching band measured across the hibschite crystal suggest a larger amount of OH in the rim relative to the core. This observation is consistent with the values calculated on the basis of stoichiometry (Table 1).

Crystal-structure refinement

Neither μXRD data (Table 2) nor single-crystal diffraction data show any evidence of symmetry lowering (*e.g.*, peak splitting or reflections violating the $Ia\bar{3}d$ systematic absences). This observation is consistent with the optically isotropic character of the

TABLE 3. F-RICH HIBSCHITE: DETAILS OF STRUCTURE REFINEMENT

Crystal size	8 × 14 × 16 μm	Total number of reflections	4669
Space group	$Ia\bar{3}d$	Reflections in Ewald sphere	2065
Unit-cell parameters		Unique reflections	71
a	12.037(3) Å	$\|Fo\| > 4\sigma_{Fo}$	54
V	1744.0(13) Å^3	R_{merge}	15.4%
Z	8	Final R_1 (unique data)	4.86%
Calculated *D*	3.274(2) g/cm^3	Final R_1 ($\|Fo\| > 4\sigma_F$)	2.84%
Linear absorption coefficient (μ)	2.45 mm^{-1}	wR_2	5.14%
		GooF	1.253
		Difference peaks	−0.30e$^-$ Å^{-3}, +0.34e$^-$ Å^{-3}

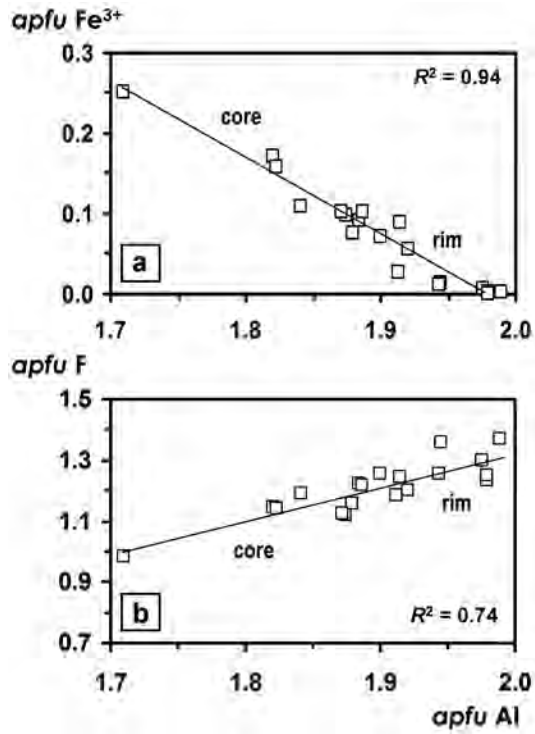

FIG. 2. Variation in Al, Fe and F contents (in *apfu* calculated to three *X*-site cations) across hibschite crystals.

hibschite crystals (*cf.* Shtukenberg *et al.* 2005). Two determinations of the unit-cell parameter derived from the μXRD and single-crystal diffraction data obtained from two different crystals are within one standard deviation of each other [12.034(3) and 12.037(3) Å, respectively]. The crystal-structure refinement in space group $Ia\bar{3}d$ was routine and converged to an R_1 of 2.8%. Because the *X* and *Y* sites in the garnet studied are occupied almost entirely by Ca and Al, respectively (Table 1), only the occupancy of the tetrahedrally coordinated *Z* site was refined along with other structural parameters. The refined Si content in the *Z* site is 2.05(5) *apfu*, which is close to the value calculated for the "bulk" crystal on the basis of the relative contributions to its volume from individual zones (1.97 *apfu*). The structural parameters and selected interatomic distances for the F-rich hibschite are reported in Table 4. A table of calculated and observed structure-factors is available from the Depository of Unpublished Data on the MAC website (document Hibschite CM46_1033).

Discussion

Crystal chemistry

The studied material is unique in that it has the highest F content reported for garnet-group minerals to date (Table 5). Unlike most of the previously described F-rich garnets, it corresponds to hibschite, *i.e.*, an intermediate member of the grossular–katoite series (Grs–Kt). Hibschite was first described from metamorphosed marl xenoliths included in phonolite at Mariánská hora in Ústí nad Labem, northwestern Czech Republic (Cornu 1906). At the type locality, hibschite is free of detectable F and occurs as small transparent crystals of octahedral morphology with H_2O-bearing andradite in their core. The crystal chemistry of this garnet was re-investigated in detail by Rinaldi & Passaglia (1989), Dvořák *et al.* (1999) and Ulrych *et al.* (2000). Hibschite is not uncommon in calcareous metamorphic rocks (see, *e.g.*, bibliography in Pertlik 2003), although most of the data available for this mineral in the literature are limited to paragenetic descriptions and (commonly incomplete) chemical analyses.

With two exceptions, all cases of F-rich garnet described in the literature to date are members of the andradite–grossular (Adr–Grs) series with <10 mol.% Kt (Table 5). If all F in the Afrikanda hibschite is assigned to the hypothetical end-member $Ca_3Al_2F_{12}$ (Fgr), its entire compositional range may be expressed as $Grs_{57–63}Kt_{21–27}Fgr_{8–11}Adr_{0–13}$. The "bulk" average composition, calculated on the basis of the volumetric proportion of individual zones (Table 1), corresponds to $Grs_{63}Kt_{24}Fgr_{10}Adr_3$. The only other known occurrence of F-rich hibschite is the Puńców sill in the Western Carpathians (Włodyka & Karwowski 2006). This mineral contains the highest Fgr content reported for any granditic garnet in the literature (*ca.* 6.7 mol.%, Włodyka & Karwowski 2006). Calcium–Fe-bearing spessartine associated with hydrothermal Mo mineralization at the Henderson mine (Smyth *et al.* 1990) and Jaguaruna (Barbanson & Bastos Neto 1992) is the only non-granditic garnet containing appreciable levels of F (on average, 8 and 2 mol.% Fgr, respectively).

The substitution of four $(OH)^-$ anions for a $(SiO_4)^{4-}$ group in granditic garnet has been studied extensively, and the structural parameters of the members of the Grs–Kt series have been well constrained (Lager *et al.* 1989, Rossman & Aines 1991, Nobes *et al.* 2000, Ferro *et al.* 2003, Orlando *et al.* 2006, among many others). The *Z*–O (center-to-corner) and O–O (corner-to-corner) distances in the ZO_4 tetrahedron are most sensitive to the "hydrogarnet" substitution; in F-free members of the Grs–Kt series, these distances closely follow the empirical relations: $Z–O = –0.107 \times Si_{apfu} + 1.955$ and $|O–O|_{tet} = –0.174 \times Si_{apfu} + 3.192$ (Fig. 4). From Table 4 and Figure 4, it is clear that the *Z*–O and $|O–O|_{tet}$ distances calculated for the Afrikanda hibschite using these equations are appreciably longer than the measured values. These discrepancies stem from the

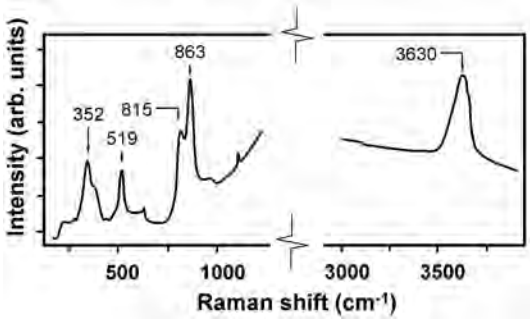

FIG. 3. Raman spectrum of F-rich hibschite showing lattice modes (including Si–O stretching bands at 815 and 863 cm^{-1}) and OH stretching modes at ~3630 cm^{-1}.

TABLE 4. F-RICH HIBSCHITE: STRUCTURAL PARAMETERS AND KEY INTERATOMIC DISTANCES

Site	Coordinates	U_{eq}	Interatomic distances (Å)	
Ca	(0, 1/4, 1/8)	0.0164(13)	Ca–O (×4)	2.351(5)
Y†	(0, 0, 0)	0.0154(15)	Ca–O (×4)	2.511(5)
Z‡	(3/8, 0, 1/4)	0.011(3)	|Ca–O|	2.431(5)
			Y–O (×6)	1.929(4)
O*		0.020(2)	*Z*–O (×4)	1.711(4)
x	0.0460(4)		$\|O–O\|_{tet}$	2.793(5)
y	0.1493(4)		$(Z–O)_{calc}$ §	1.736
z	–0.0359(4)		$\|O–O\|_{tet,\ calc}$ §	2.835

† *Y* = $(Al_{0.97}Fe_{0.03})$ from EMPA; ‡ *Z*-site occupancy refined from single-crystal X-ray-diffraction data is 2.05(5) *apfu* (*cf.* 1.97 *apfu* from EMPA); * O-site occupancy is $(O_{0.9}F_{0.1})$ from EMPA; § distances are calculated assuming only oxygen at the O site.

TABLE 5. FLUORINE-BEARING GARNETS: A SUMMARY OF PUBLISHED DATA (ARRANGED CHRONOLOGICALLY)

Mineral	wt.%F *apfu* F	Other compositional characteristics §‡	Paragenesis	Locality	Additional data† Reference
Hibschite	4.2-6.0 0.98-1.37	≤4.6 wt.% Fe_2O_3	Low-temperature hydro-thermal in silicocarbonatite	Afrikanda, Kola,Russia	XRD,SCSR,Raman This work
Hibschite ~14 mol.% Kt	3.5 0.80	0.22 *apfu* Fe^{3+}	Metasomatic, altered nepheline syenite	Puńców sill, Poland	Raman Włodyka & Karwowski (2006)
Borderline andradite-grossular	0.5-1.6 0.12-0.41	0.4-0.5 wt.%MnO, 0.2-2.3 wt.%TiO_2	Low-grade metamorphic after tonalite–granodiorite	Malá Fatra Mts. Slovakia	None Faryad & Dianiška (2003)
Andradite with 25-31 mol.% Grs	0.5-2.0 0.12-0.48	1.3-2.3 wt.% TiO_2	Low-grademetamorphic after gabbroic and granitic rocks	Charroux-Civray, France, Fichtel-gebirge, Germany	None Freiberger *et al.* (2001)
Andradite with 9-19 mol.% Grs	0.1-0.5 0.03-0.12	0.2-1.0 wt.% MgO, 1.4-3.7 wt.% TiO_2	Metasomatic melilitolitic pegmatite	Osečná, Czech Republic	POP, UCP, WG, MS, TE Ulrych *et al.* (1994)
Borderline andradite-grossular	0.1-1.6 0.03-0.40	≤0.9 wt.% TiO_2	Low-grade metamorphic	Blengsvatn, Norway	UCP Visser (1993)
Borderline andradite-grossular	4.6 (max.) 0.78 (mean)	2.8 wt.% TiO_2	Hydrothermal after amphibole--biotite granite	Pedras Grandes, Santa Catarina, Brazil	None / Barbanson & Bastos Neto (1992)
Spessartine	1.9 (max) 0.23 (mean)	12.7 wt.% CaO, 11.7 wt.%FeO	Leucogranite, associated with Mo mineralization	Jaguaruna, Santa Catarina,Brazil	None / Barbanson & Bastos Neto (1992)
Spessartine	3.2-4.3 0.97 (mean)	0.6 wt.% CaO, 4.8 wt.% FeO	Hydrothermal, associated with Mo mineralization	Henderson mine, Colorado,USA	SCSR, IR Smyth *et al.* (1990)
Andradite-grossular (complete range)	0-2.7 0.64 (max)	≤1.6 wt.% TiO_2, ≤1.0 wt.% MnO	Retrograde metamorphic aftercontact-metamorphic wollastonite–hedenbergite	Skaergaard, East Greenland	None Manning & Bird (1990)
Borderline andradite-grossular	1.0-3.1 ~0.2-0.7*	1.8-3.4 wt.% TiO_2	Metasomatized ijolite	Magnet Cove Arkansas, USA	UCP Flohr & Ross (1989)
Grossular	0.2-0.8 0.18 (max)	~1.3 wt.% Fe_2O_3	Retrograde metamorphic after wollastonite in calc-silicate rocks	Lake Bonaparte, and Port Leyden, New York, USA	UCP, optics Valley *et al.* (1983)

§ All F and oxide contents listed in this Table were obtained by electron-microprobe analysis. ‡ Only major elements (present in concentrations ≥ 0.5 wt.%) are listed. XRD: X-ray-diffraction pattern, SCSR: single-crystal structure refinement, POP: physical and optical properties, UCP: unit-cell parameter(s), WG: H_2O by gravimetry, MS: Mössbauer spectroscopic data, TE: trace-element analysis, IR: infrared spectroscopic data. * The *apfu* numbers are approximate because the analytical data do not recalculate well to structural formulae. Symbols used: Grs: grossular, Kt: katoite.

smaller ionic radius of F^- relative to O^{2-} (Shannon 1976) and, consequently, the smaller size of the F_4^{4-} tetrahedron relative to the $(OH)_4^{4-}$ tetrahedron. Using the refined occupancy of the *Z* site and the empirically constrained variations of *Z*–O and lO–Ol_{tet} along the Grs–Kt join (Fig. 4), we estimate that the F_4^{4-} tetrahedron has an average edge-length of ~3.08 Å and a center-to-corner distance of ~1.85 Å. The edge length and center-to-corner distance in the structure of pure katoite are 3.20 and 1.96 Å, respectively (Lager *et al.* 1987).

Conditions of crystallization

The F-rich hibschite is a product of postmagmatic hydrothermal activity, which gave rise to a late-stage assemblage of minerals overprinting the primary magmatic assemblage (calcite, magnesiohastingsite, diopside, perovskite and ilmenite) and developed predominantly in fractures within the silicocarbonatite. The fracturing probably occurred during the same hydrothermal event (for example, in response to CO_2 ebullition) as the deposition of hibschite and other late-

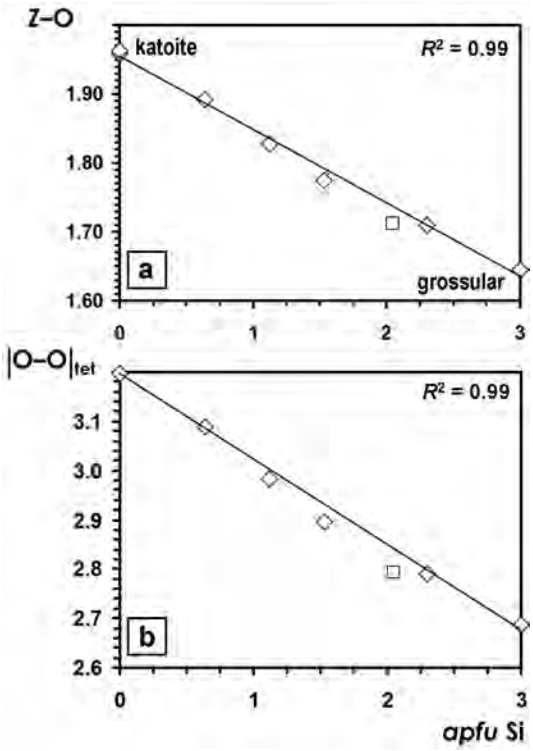

FIG. 4. Variation in key interatomic distances (in Å) with increasing proportion of Si at the *Z* site in Ca–Al "hydrogarnet": (a) center-to-corner distance in the ZO_4 tetrahedron; (b) average corner-to-corner distance in the ZO_4 tetrahedron. Diamonds correspond to published data for the grossular–katoite series (Basso *et al.* 1983, Sacerdoti & Passaglia 1985, Lager *et al.* 1987, 1989, Geiger & Armbruster 1997, Prodjosantoso *et al.* 2002, Ferro *et al.* 2003), and square corresponds to the data for F-rich hibschite (this work). In all cases, the error bars are smaller than, or comparable to, the size of the symbols.

stage minerals. On the basis of textural and paragenetic relations, the conditions of hibschite crystallization correspond to *T* in the interval 250–300°C, log $f(CO_2) \approx -1.0$, log $a(H_4SiO_4)_{aq} \geq -4$ and log $a(H^+) \approx -5$ (Chakhmouradian 2004, Chakhmouradian & Zaitsev 2004). Our temperature estimate is consistent with the published estimates for F-bearing granditic garnet with less than 10 mol.% Kt (300–400°C at *P* in the range 1–4 kbar: Visser 1993, Freiberger *et al.* 2001, Faryad & Dianiška 2003).

Elevated levels of F are not uncommon in carbonatites, some of which contain economic concentrations of fluorite (Palmer & Williams-Jones 1996, Bühn *et al.* 2002). In the absence of fluorite, F is disseminated in Mg–Fe micas and amphiboles (up to 3.2 wt.% F for both: Hogarth 1989, Lee *et al.* 2004), apatite (up to 4.8 wt.% F: Bühn *et al.* 2001), pyrochlore-group minerals (up to 5.6 wt.% F: Lee *et al.* 2004) and fluorocarbonates (up to 7.9 wt.% F in bastnäsite: Wall & Zaitsev 2004). Although F-rich garnet was unknown from carbonatites prior to this work, granditic garnet with up to 3.1 wt.% F has been reported from metasomatized alkaline rocks affected by carbonatite-derived fluids (Flohr & Ross 1989, Ulrych *et al.* 1994; Table 5). Hence, the enrichment of hibschite at Afrikanda in F is not entirely unexpected. It is, however, remarkable that this garnet is the *principal* host of F in the paragenesis examined because none of the aforementioned F-bearing minerals occurs in the same association.

Neither the silicocarbonatite nor its metasomatized milieu contains any fluorite. Given that the activity of Ca^{2+} remained high throughout the postmagmatic stage of crystallization, the absence of fluorite at Afrikanda must imply insufficient $a(F^-)$ in the fluid. Manning & Bird (1990) analyzed phase relations between F-bearing grossular and fluorite in metasomatic calc-silicate rocks and concluded that the composition of garnet is sensitive to the composition of the fluid and can be used to constrain log $[a(H^+) \times a(F^-)]$ in that fluid. Using Equation 17b of Manning & Bird (1990), we estimate that the Afrikanda hibschite crystallized at a log $[a(H^+) \times a(F^-)]$ value of –10 [*i.e.*, log a (F^-) around –5]. The documented increase in F content from the core of hibschite crystals rimward (Table 1, Fig. 2b) indicates either a drop in temperature or an increase in log $a(F^-)$ between the two temporally separated episodes of growth (core and rim).

ACKNOWLEDGEMENTS

This work was inspired by John Gittins's lasting contribution to the study of silicocarbonatites and their fascinating minerals. Our project was supported financially by the Natural Sciences and Engineering Research Council of Canada, Canada Foundation for Innovation, and University of Manitoba. Panseok Yang is thanked for his skilled help with the acquisition of electron-microprobe data. This paper benefitted from many useful comments made on its earlier version by Jaromír Ulrych, Evgeny Galuskin and Editor Robert F. Martin.

REFERENCES

ARREDONDO, E.H. & ROSSMAN, G.R. (2002): Feasibility of determining the quantitative OH content of garnets with Raman spectroscopy. *Am. Mineral.* **87**, 307-311.

BARBANSON, L. & BASTOS NETO, A.C. (1992): Hydroandradite titanifère fluorée et grenat ($Spe_{39}Gro_{31}Alm_{23}And_6$) fluoré des granitoïdes du district à fluorine de Santa Catarina (Brésil): description minéralogique, mécanisme d'incorporation du fluor, signification pétrologique et métallogénique. *C.R. Acad. Sci. Paris, Sér. II* **314**, 63-69.

BASSO, R., DELLA GIUSTA, A. & ZEFIRO, L. (1983): Crystal structure refinement of plazolite: a highly hydrated natural hydrogrossular. *Neues Jahrb. Mineral., Monatsh.*, 251-258.

BROD, J.A., JUNQUEIRA-BROD, T.C., GASPAR, J.C., GIBSON, S.A. & THOMPSON, R.N. (2003): Ti-rich and Ti-poor garnet from the Tapira carbonatite complex, SE Brazil: fingerprinting fractional crystallization and liquid immiscibility. *In* 8th International Kimberlite Conference, Extended Abstracts (CD), FLA_0339.pdf.

BÜHN, B., RANKIN, A.H., SCHNEIDER, J. & DULSKI, P. (2002): The nature of orthomagmatic, carbonatitic fluids precipitating REE,Sr-rich fluorite: fluid-inclusion evidence from the Okorusu fluorite deposit, Namibia. *Chem. Geol.* **186**, 75-98.

BÜHN, B., WALL, F. & LE BAS, M.J. (2001): Rare-earth element systematics of carbonatitic fluorapatites, and their significance for carbonatite magma evolution. *Contrib. Mineral. Petrol.* **141**, 572-591.

CHAKHMOURADIAN, A.R. (2004): Crystal chemistry and paragenesis of compositionally unique (Al-, Fe-, Nb, and Zr-rich) titanite from Afrikanda, Russia. *Am. Mineral.* **89**, 1752-1762.

CHAKHMOURADIAN, A.R. & MCCAMMON, C.A. (2005): Schorlomite: a discussion of the crystal chemistry, formula, and inter-species boundaries. *Phys. Chem. Minerals* **32**, 277-289.

CHAKHMOURADIAN, A.R. & ZAITSEV, A.N. (2002): Calcite – amphibole – clinopyroxene rock from the Afrikanda complex, Kola Peninsula, Russia: mineralogy and a possible link to carbonatites. III. Silicate minerals. *Can. Mineral.* **40**, 1347-1374.

CHAKHMOURADIAN, A.R. & ZAITSEV, A.N. (2004): Afrikanda: an association of ultramafic, alkaline and alkali-silica-rich carbonatitic rocks from mantle-derived melts. *In* Phoscorites and Carbonatites from Mantle to Mine: the Key Example of the Kola Alkaline Province (F. Wall & A.N. Zaitsev, eds.). Mineralogical Society, London, U.K. (247-291).

CORNU, F. (1906): Beiträge zur Petrographie des Böhmischen Mittelgebirges. I. Hibschit, ein neues Kontaktmineral. *Tschermaks Mineral. Petrogr. Mitt.* **25**, 249-268.

DVOŘAK, Z., JANEČEK, O., PAULIŠ, P. & ŘEHOŘ, M. (1999): Hibschite (hydrogrossular) from the quarry of Mariánská hora Hill at Ustí nad Labem. *Bull. Mineral.-Petrogr. Odd. Nár. Muz. Praze* **7**, 236 (in Czech).

FARYAD, S.W. & DIANIŠKA, I. (2003): Ti-bearing andradite – prehnite – epidote assemblage from the Malá Fatra granodiorite and tonalite (western Carpathians). *Schweiz. Mineral. Petrogr. Mitt.* **83**, 47-56.

FERRO, O., GALLI, E., PAPP, G., QUARTIERI, S., SZAKÁLL, S. & VEZZALINI, G. (2003): A new occurrence of katoite and re-examination of the hydrogrossular group. *Eur. J. Mineral.* **15**, 419-426.

FLOHR, M.J.K. & ROSS, M. (1989): Alkaline igneous rocks of Magnet Cove, Arkansas: mjetasomatized ijolite xenoliths from Diamond Jo quarry. *Am. Mineral.* **74**, 113-131.

FREIBERGER, R., HECHT, L., CUNEY, M. & MORTEANI, G. (2001): Secondary Ca–Al silicates in plutonic rocks: implications for their cooling history. *Contrib. Mineral. Petrol.* **141**, 415-429.

GEIGER, C.A. & ARMBRUSTER, T. (1997): $Mn_3Al_2Si_3O_{12}$ spessartine and $Ca_3Al_2Si_3O_{12}$ grossular garnet: structural dynamic and thermodynamic properties. *Am. Mineral.* **82**, 740-747.

HOGARTH, D.D. (1989): Pyrochlore, apatite and amphibole: distinctive minerals in carbonatite. *In* Carbonatites: Genesis and Evolution (K. Bell, ed.). Unwin Hyman, London, U.K. (105-148).

HOLLAND, T.J.B. & REDFERN, S.A.T. (1997): Unit cell refinement from powder diffraction data: the use of regression diagnostics. *Mineral. Mag.* **61**, 65-77.

IBERS, J.A. & HAMILTON, W.C., eds. (1992): *International Tables for X-ray Crystallography* **IV**. Kynoch Press, Birmingham, U.K.

LAGER, G.A., ARMBRUSTER, T. & FABER, J. (1987): Neutron and X-ray diffraction study of hydrogarnet $Ca_3Al_2(O_4H_4)_3$. *Am. Mineral.* **72**, 756-765.

LAGER, G.A., ARMBRUSTER, T., ROTELLA, F.J. & ROSSMAN, G.R. (1989): OH substitution in garnets: X-ray and neutron diffraction, infrared, and geometric-modeling studies. *Am. Mineral.* **74**, 840-851.

LEE, M.J., GARCIA, D., MOUTTE, J., WILLIAMS, C.T. & WALL, F. (2004): Carbonatites and phoscorites from the Sokli complex, Finland. *In* Phoscorites and Carbonatites from Mantle to Mine: the Key Example of the Kola Alkaline Province (F. Wall & A.N. Zaitsev, eds.). Mineralogical Society, London, U.K. (133-162).

LUPINI, L., WILLIAMS, C.T. & WOOLLEY, A.R. (1992): Zr-rich garnet and Zr- and Th-rich perovskite from the Polino carbonatite, Italy. *Mineral. Mag.* **56**, 581-586.

MANNING, C.E. & BIRD, D.K. (1990): Fluorian garnets from the host rocks of the Skaergaard intrusion: implications for metamorphic fluid composition. *Am. Mineral.* **75**, 859-873.

NOBES, R.H., AKHMATSKAYA, E.V., MILMAN, V., WINKLER, B. & PICKARD, C.J. (2000): Structure and properties of aluminosilicate garnets and katoite: an ab initio study. *Comput. Mater. Sci.* **17**, 141-145.

ORLANDO, R., TORRES, F.J., PASCALE, F., UGLIENGO, P., ZICOVICH-WILSON, C. & DOVESI, R. (2006): Vibrational spectrum of katoite $Ca_3Al_2[(OH)_4]_3$: a periodic ab initio study. *J. Phys. Chem. B* **110**, 692-701.

PALMER, D.A.S. & WILLIAMS-JONES, A.E. (1996): Genesis of the carbonatite-hosted fluorite deposit at Amba Dongar, India: evidence from fluid inclusions, stable isotopes, and whole rock – mineral geochemistry. *Econ. Geol.* **91**, 934-950.

PERTLIK, F. (2003): Bibliography of hibschite, a hydrogarnet of grossular type. *GeoLines* **15**, 113-119.

PRODJOSANTOSO, A.K., KENNEDY, B.J. & HUNTER, B.A. (2002): Phase separation induced by hydration of the mixed Ca/Sr aluminates $Ca_{3-x}Sr_xAl_2O_6$. A crystallographic study. *Cement Concr. Res.* **32**, 647-655.

RINALDI, R. & PASSAGLIA, E. (1989): Hibschite topotype: crystal chemical characterization. *Eur. J. Mineral.* **1**, 639-644.

ROSSMAN, G.R. & AINES, R.D. (1991): The hydrous component in garnets: grossular–hydrogrossular. *Am. Mineral.* **76**, 1153-1164.

SACERDOTI, M. & PASSAGLIA, E. (1985): The crystal structure of katoite and implications within the hydrogrossular group of minerals. *Bull. Minéral.* **108**, 1-8.

SHANNON, R.D. (1976): Revised effective ionic radii and systematic studies of interatomic distances in halides and chalcogenides. *Acta Crystallogr.* **A32**, 751-767.

SHELDRICK, G.M. (1997): SHELX-97: *Program for the Solution and Refinement of Crystal Structures*. Siemens Energy and Automation, Madison, Wisconsin.

SHTUKENBERG, A.G., POPOV, D.YU. & PUNIN, YU.O. (2005): Growth ordering and anomalous birefringence in ugrandite garnets. *Mineral. Mag.* **69**, 537-550.

SMYTH, J.R., MADEL, R.E., MCCORMICK, T.C., MUNOZ, J.L. & ROSSMAN, G.R. (1990): Crystal-structure refinement of a F-bearing spessartine garnet. *Am. Mineral.* **75**, 314-318.

ULRYCH, J., NOVÁK, J.K., LANGROVÁ, A., MELKA, K., CAJZ, V., ADAMOVIČ, J., PERTLIK, F., WIESNER, T., ŽID, L. & RADOŇ, M. (2000): Tertiary phonolite laccolith of Mariánská hora Hill, N. Bohemia: geological, petrological and mineralogical characteristics. *Acta Montana* **15**(116), 5-44.

ULRYCH, J., POVONDRA, P., PIVEC, E., RUTŠEK, J. & SITEK, J. (1994): Compositional evolution of metasomatic garnet in melilitic rocks of the Osečná complex, Bohemia. *Can. Mineral.* **32**, 637-647.

VALLEY, J.W., ESSENE, E.J. & PEACOR, D.R. (1983): Fluorine-bearing garnets in Adirondack calc-silicates. *Am. Mineral.* **68**, 444-448.

VISSER, D. (1993): Fluorine-bearing hydrogarnets from Blengsvatn, Bamble sector, south Norway. *Mineral. Petrol.* **47**, 209-218.

WALL, F. & ZAITSEV, A.N. (2004): Rare earth minerals in Kola carbonatites. *In* Phoscorites and Carbonatites from Mantle to Mine: the Key Example of the Kola Alkaline Province (F. Wall & A.N. Zaitsev, eds.). Mineralogical Society, London, U.K. (341-373).

WŁODYKA, R. & KARWOWSKI, Ł. (2006): Fluorine-bearing garnets from the teschenite sill in the Polish Western Carpathians. *Acta Mineral.-Petrogr., Abstr. Ser.* **5**, 131.

Received June 8, 2007, revised manuscript accepted July 1, 2008.